# Biologically Induced Changes in the Partitioning of Submicron Particulates Between Bulk Seawater and the Sea Surface Microlayer

**Daniel R. Crocker[*,1], Grant B. Deane[2], Ruochen Cao[1], Mitchell V. Santander[1], Clare K. Morris[2], Julie Dinasquet[2], Sarah Amiri[1], Brock A. Mitts[1], Francesca Malfatti[2,3,4], Kimberly A. Prather[1,2], Mark H. Thiemens[1]**

[1]Department of Chemistry and Biochemistry, University of California, San Diego, La Jolla, California, 92093 USA

[2]Scripps Institution of Oceanography, La Jolla, California, 92037, USA

[3]University of Trieste, Trieste 34100, Italy
[4]OGS (Istituto Nazionale di Oceanografia e di Geofisica Sperimentale), Trieste 34100, Italy

Corresponding author: Daniel Crocker (dcrocker@ucsd.edu)

**Key Points:**

- Increases in seawater submicron particulates during a phytoplankton bloom are size-dependent and influenced by the bloom phase.
- Particulate enrichment in the sea surface microlayer is low in the absence of wave breaking and bubble scavenging
- Augmented biological production of submicron particulates may enhance their entrainment in sea spray aerosol particles

## Abstract

Studies over the last two decades have shown that submicron particulates (SMPs) can be transferred from the seawater into sea spray aerosol (SSA), potentially impacting SSA cloud seeding ability. This work reports the first concurrent bulk and sea surface microlayer (SSML) SMP (0.4-1.0 μm) measurements, made during two mesocosm phytoplankton blooms in a region devoid of active wave breaking and bubble formation, providing insight into how biological and physicochemical processes influence seawater SMP distributions. Modal analyses of the SMP size distributions revealed contributions from multiple, biologically-related particulate populations that were controlled by the microbial loop. With negligible bubble scavenging occurring, SSML enrichment of SMPs remained low throughout both experiments, suggesting this process is vital for SMP enrichment in the SSML. Because many biological SMPs can induce ice formation in SSA, our findings are discussed in the context of SMP transfer into SSA and its potential importance for SSA ice nucleation.



## Plain Language Summary

Research has shown that particulates can be transferred from the ocean into sea spray aerosol (SSA) when bubbles burst at the ocean surface. This transfer is important because incorporation of seawater particulates into SSA can impact its ability to seed water and ice clouds. During the Sea Spray Chemistry and Particulate Evolution (SeaSCAPE) study, submicron particulates (SMPs, 0.4-1.0 μm) were measured daily in the sea surface microlayer (SSML), the topmost 1-1000 μm of the ocean surface, and the underlying bulk seawater over the course of two phytoplankton growth experiments. The objective of this study was to assess the influence of

biological activity on SMP concentrations and distributions in the seawater. Our results indicate that biological growth led to increased SMP production, and the size distribution of SMPs produced was dependent on the phase of the bloom growth. Additionally, almost no SSML enrichment of SMPs occurred without active wave breaking and bubble formation, highlighting the significance of biological activity and bubble scavenging/bursting for particulate transfer into SSA. Because biological SMPs in SSA can serve as sites for ice formation, these findings are discussed in the context of potential SMP impacts on SSA ice nucleation.

## 1. Introduction

Seawater submicron particulates (SMPs) are a vital component of oceanic biogeochemical processes, contributing to carbon and nutrient cycling, trophic interactions, and attenuation of sunlight (Jonasz & Fournier, 2007; Verdugo, 2012). Research over the last two decades has additionally revealed that SMPs can be entrained in sea spray aerosol (SSA) (Bigg & Leck, 2008; Facchini et al., 2008; Leck & Bigg, 2005). The compositional changes that arise from SMP entrainment in SSA can have climatically important impacts on its hygroscopicity, cloud condensation nuclei activity, and ability to serve as ice-nucleating particles (INPs) in the atmosphere (Bigg & Leck, 2001; Després et al., 2012; Orellana et al., 2011).

The potential contribution of SMPs to seawater ice-nucleating entities (INEs) is especially intriguing, as only about 1 in every $10^5$ SSA particles serve as INPs (DeMott et al., 2016). Previous research has shown that seawater particulates (>0.2 μm) can comprise over 80% of bulk seawater INEs (McCluskey et al., 2018). Micro-Raman spectroscopy on individual SSA particles collected from this study revealed that INPs with diameters from 0.56-1.0 μm primarily contained siliceous phytoplankton material, providing evidence that biologically-related SMPs contribute to SSA

INPs. This size range is particularly interesting because multiple studies have reported elevated 0.4-0.7 μm SMPs in biologically-active bulk seawater (Isao et al., 1990; Longhurst et al., 1992; Yamasaki et al., 1998). These SMPs have been correlated with chlorophyll-a (chl-a), bacteria, and heterotrophic nanoflagellate concentrations (Yamasaki et al., 1998), but the primary biological parameter driving their formation has not been identified. Because the 0.4-0.7 μm SMP size mode is associated with microbial activity, it will hereafter be referred to as the "microbial mode".

Monitoring evolution of the microbial mode throughout an entire phytoplankton bloom would be beneficial to identify the biological contributors to the microbial mode. A number of studies have found that seawater biological INEs, including diatoms, heterotrophic bacteria, and their cell fragments, constitute a significant portion of SSA INPs (Knopf et al., 2011; McCluskey et al., 2018; Tesson & Šantl-Temkiv, 2018). Therefore, elucidating the biological components comprising microbial mode SMPs may help explain elevated seawater INE concentrations during phytoplankton blooms (McCluskey et al., 2018; Mitts et al., 2021), providing insight into the higher concentrations of SSA INPs produced from biologically-active seawater (Creamean et al., 2019; DeMott et al., 2016; Mitts et al., 2021; Wolf et al., 2020).

Transfer of biological INEs into SSA also depends on physical processes such as bubble scavenging of organic material and the bubble bursting mechanisms that form SSA. SSA is produced both from the bubble film cap when it bursts at the air-sea interface and from the bubble's base during subsequent collapse of the bubble cavity (Wang et al., 2017). It follows that particulate transfer into SSA will be influenced by particulate concentrations in the sea surface microlayer (SSML), the top 1-1000 μm of the ocean surface often enriched in biological components and organic material (Aller et al., 2005; Bigg et al., 2004; Wurl et al., 2011), as well as particulate concentrations in the underlying bulk seawater. Therefore, assessing ocean-aerosol

transfer of microbial mode SMPs necessitates SMP measurements in both the bulk and SSML; however, simultaneous size measurements of bulk and SSML particulates have primarily focused on supermicron particulates (Stramski et al., 2019).

This work reports the first concurrent particle size distribution measurements for 0.4-1.0 μm SMPs in the bulk seawater and SSML made throughout two phytoplankton bloom mesocosm experiments to elucidate how biological activity influences the distribution and concentration of SMPs between the bulk seawater and SSML. The measurements were made in a region far downstream from active wave breaking and bubble formation, providing insight on SMP partitioning between the bulk and SSML when bubble scavenging was minimal. Our results are discussed in the context of ocean-aerosol SMP transfer and the potential contribution of SMPs to SSA ice nucleation.

## 2. Materials and Methods

### 2.1. The Wave Channel Mesocosm Experiments

Two mesocosm experiments were conducted in an ocean-atmosphere wave channel at the SIO Hydraulics Laboratory as part of the 2019 Sea Spray Chemistry and Particulate Evolution (SeaSCAPE) study. A wave channel depiction and detailed description of experimental and biological parameters can be found in Sauer et al. (2021). For both experiments, the 11,800 L wave channel was filled with natural, filtered seawater (50 μm Nitex mesh) collected from the coastal Pacific Ocean. Experiment 1 achieved a full phytoplankton bloom growth and decay cycle from July 1$^{st}$-July 10$^{th}$, after the addition of f/2 diatom growth nutrients on July 4$^{th}$ (Guillard & Ryther, 1962). For Experiment 2, from July 12$^{th}$-July 19$^{th}$, a more dilute f/20 nutrient mixture was added, and little phytoplankton growth was observed over the course of the experiment

(Figure S1a). For completeness, we report SMP measurements from Experiment 2 (Figure 1, Figure S1b), however because a phytoplankton bloom did not occur, most discussion about Experiment 2 has been placed in the Supporting Information (SI, Text S1).

### 2.2. Seawater Sampling and Biological Measurements

All seawater measurements, including *in situ* measurement of chl-a to monitor phytoplankton growth, were made at the back of the wave channel in a designated seawater sampling section (Sauer et al. 2021). Once daily in the seawater sampling section, 16 L of bulk seawater was siphoned from the wave channel and 200 mL of SSML was collected using the glass plate method (Carlson, 1982; Cunliffe & Wurl, 2015). A 1.5 mL aliquot of each sample was taken for PSD analysis, and aliquots from the same bulk seawater were used for bacteria and virus enumeration. More information on quantification of chl-a, bacteria, and viruses is provided in SI Text S2. Separately, a 50 mL aliquot was collected each day to enumerate phytoplankton using the Utermöhl method (Figure S2, Utermöhl, 1958).

The seawater sampling section was located about 20 meters downstream from the active wave breaking region. The wave channel surface water flow is about 1 cm per minute, so surface waters would take around 30 minutes to transit from the wave breaking region to the seawater sampling section. Because of the long time duration between wave breaking and seawater sample collection, we are interpreting the particulate measurements to be reflective of seawater conditions where the effects of active wave breaking and bubble scavenging are negligible.

### 2.3. Particulate Size Measurements and Analysis

#### 2.3.1. Multispectral Advanced Nanoparticulate Tracking Analysis (MANTA)

Particulates were sized using a MANTA ViewSizer® 3000 (Horiba Scientific). Individual particulates in the seawater sample are illuminated by three lasers at separate wavelengths and their Brownian motion is simultaneously tracked by a video camera. The MANTA software uses the Brownian motion to determine the diffusion coefficient (D) of each individual particulate. Under the assumption that particulates are spherical, the hydrodynamic diameter ($d_h$) is calculated from the measured diffusion coefficient using the Stokes-Einstein equation (Einstein, 1905):

$$d_h = \frac{k_B T}{3\pi\eta D} \qquad (1)$$

In Equation 1, $k_B$ is the Boltzmann constant, T is seawater temperature, and $\eta$ is seawater viscosity. Although the MANTA specifically measures hydrodynamic diameters, this work reports equivalent spherical diameters (ESDs). In addition to assuming spherical particulates, ESD assumes particulates exhibit identical hydrodynamic, optical, electrical, and aerodynamic properties, allowing for comparison between different sizing techniques (McNaught & Wilkinson, 2019).

In our experiments, the MANTA reported particulates with $d_h$ from 0.01-1.0 μm. However, detection of the smallest particulates strongly depends on the refractive index contrast between the particulate and seawater medium, which was not measured. Therefore, we focused this study on seawater particulate sizes ranging from 0.4-1.0 μm. Further details on MANTA operating conditions and software determination of $d_h$ are provided in SI Text S3.

### 2.3.2. Particulate Size Distributions

The role of particulates in surface ocean processes often depends on their concentration and size distribution (Groundwater et al., 2012). The particulate size distribution (PSD), represented by $N'(d)$ in Equation 2a, is best described as the average number of particulates per unit volume of seawater, N(d), in a given diameter range (Δd) (Reynolds et al., 2010).

$$N'(d) = \frac{N(d)}{\Delta d} \qquad (2a)$$

$$N'(d) = N_o(d)^{\xi} \qquad (2b)$$

Frequently a portion of seawater PSDs, or the entire distribution, follow a general power law distribution of the form in Equation 2b, where $N_o$ is the differential number concentration, and $\xi$ represents how quickly particulate concentrations decrease with increasing diameter (Reynolds et al., 2010). In a loglog plot of d vs. N'(d), $\xi$ is equal to the PSD slope (see Section 3.1 below).

### 2.3.3 Modal Analyses of PSDs

Lognormal modal analyses of the PSDs were performed in MATLAB software using maximum likelihood estimates (MLE) for parameters of a normal distribution. Although particulate sizes overall do not follow a lognormal distribution, lognormal analysis has been previously used to identify modal contributions to the total PSD (Jonasz & Fournier, 1996; Zhang et al., 2011). This analysis is motivated by the fact that many particulate populations such as phytoplankton, bacteria, nonliving organic matter, and mineral particulates follow lognormal distributions in the ocean (Jonasz & Fournier, 2007). We recognize there are many possible ways to fit modal analyses to our PSD data. Because our goal was to assess particulate populations contributing to the microbial mode, we chose to decompose each PSD into four lognormal modes with constraints placed on the means and standard deviations. Four modes were sufficient to accurately reproduce the measured PSDs while still resolving particulate populations.

# 3. Results and Discussion

## 3.1. Seawater Submicron PSDs

Comparing our PSD measurements with previous oceanic SMP studies is difficult because the oceanic PSD slopes vary widely from -3 to -10 (Figure 1, Babin et al., 2012; Gallego-Urrea et al., 2010; Wells & Goldberg, 1992, 1994; Yamasaki et al., 1998; Zhang et al., 2012). The cause of this variability is uncertain, but may result from analytical limitations that restrict most measurements to only a portion of SMP sizes (Groundwater et al., 2012). To provide better context for our measurements, the previously measured oceanic PSDs in Figure 1 have been averaged at 0.05 µm intervals over the 0.05-1.0 µm range and plotted as open circles along with gray dashed lines for the 95% confidence interval. The averaged values are well represented by a power law function (solid black line, $R^2 = 0.94$) with a PSD slope of -3.72, similar to the value observed for combined submicron and supermicron marine detritus (-3.36, Jonasz & Fournier 2007), and within the commonly reported -3 to -4 range for supermicron PSDs (Reynolds et al., 2010; Runyan et al., 2020). Thus, despite PSD slope inconsistency over segments of the SMP size range, a power law distribution with a PSD slope similar to supermicron particulates likely provides a good approximation for oceanic SMP concentrations when assessing the full 0.05-1.0 µm range.

The bulk and SSML PSD measurements for Experiments 1 and 2, averaged using each day of both experiments, are overlaid on the bulk seawater oceanic PSDs in Figure 1. All four PSDs fall within the 95% confidence interval calculated from the averaged oceanic values, and are on the same order of magnitude as previous Pacific Ocean measurements in coastal San Diego (solid maroon lines). Additionally, the microbial mode between 0.4-0.7 µm, where the PSD deviates from the typical power law decrease, is clearly visible (and labeled) in Figure 1 for all four PSDs in this study as well as the averaged oceanic values.

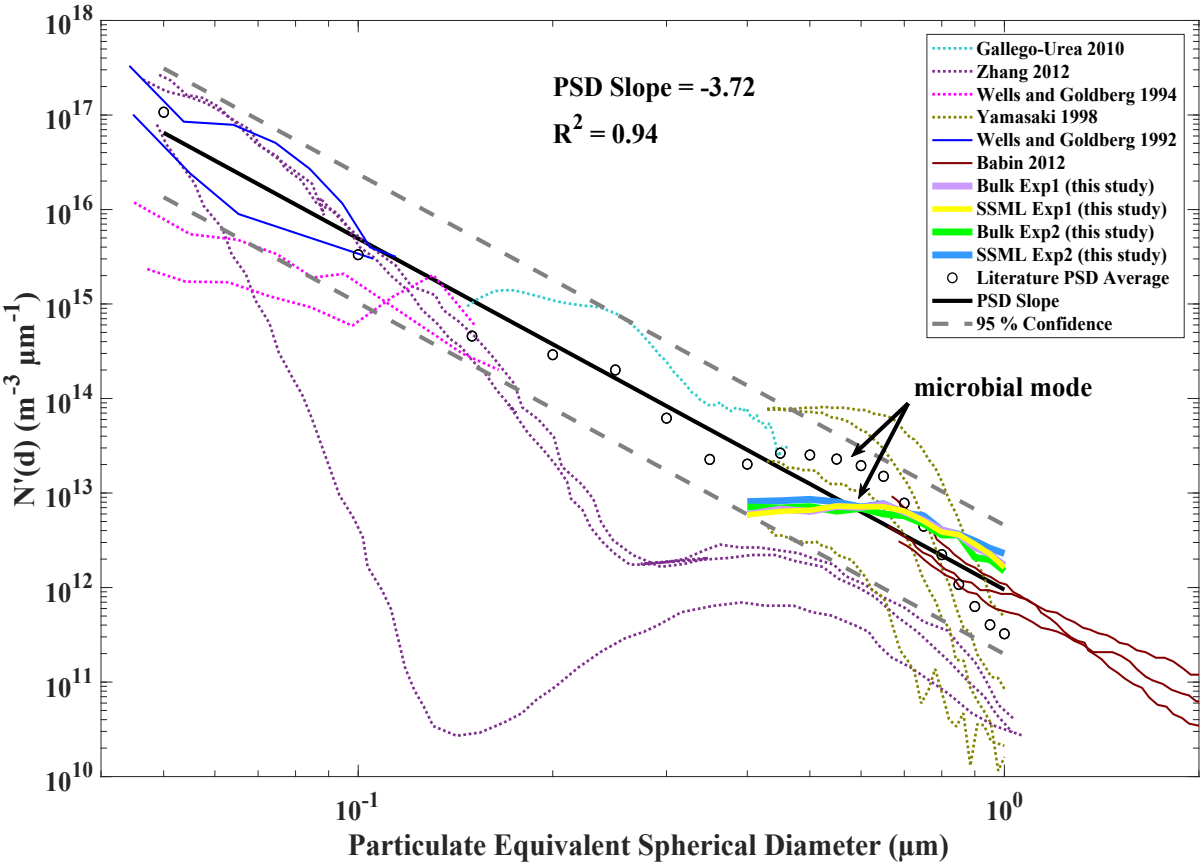


**Figure 1.** Bulk and SSML PSDs from both mesocosm experiments in this study, plotted along with previously reported bulk seawater oceanic PSDs. Solid lines represent PSDs measured for coastal San Diego seawater, while dotted lines represent measurements in other oceanic regions. All four PSDs from this study fell within the 95% confidence interval (gray dashed lines) calculated for the averaged oceanic values.

### 3.2. Evolution of Biology and Particulate Concentrations During Experiment 1

Experiment 1 followed the typical bloom progression with phytoplankton growth (chl-a) increasing after addition of the diatom growth nutrients. The phytoplankton population also shifted from a mixed community to diatom dominated as the bloom progressed (Figure S2). Phytoplankton growth was closely followed by elevated bacteria concentrations, and then higher

virus concentrations in response to the bacteria (Figure 2a, Azam et al., 1983; Lee et al., 2015). To evaluate the role of biology on SMP concentrations, the experiment was separated into "pre-bloom", "growth", and "decay" phases (labeled in Figure 2a).

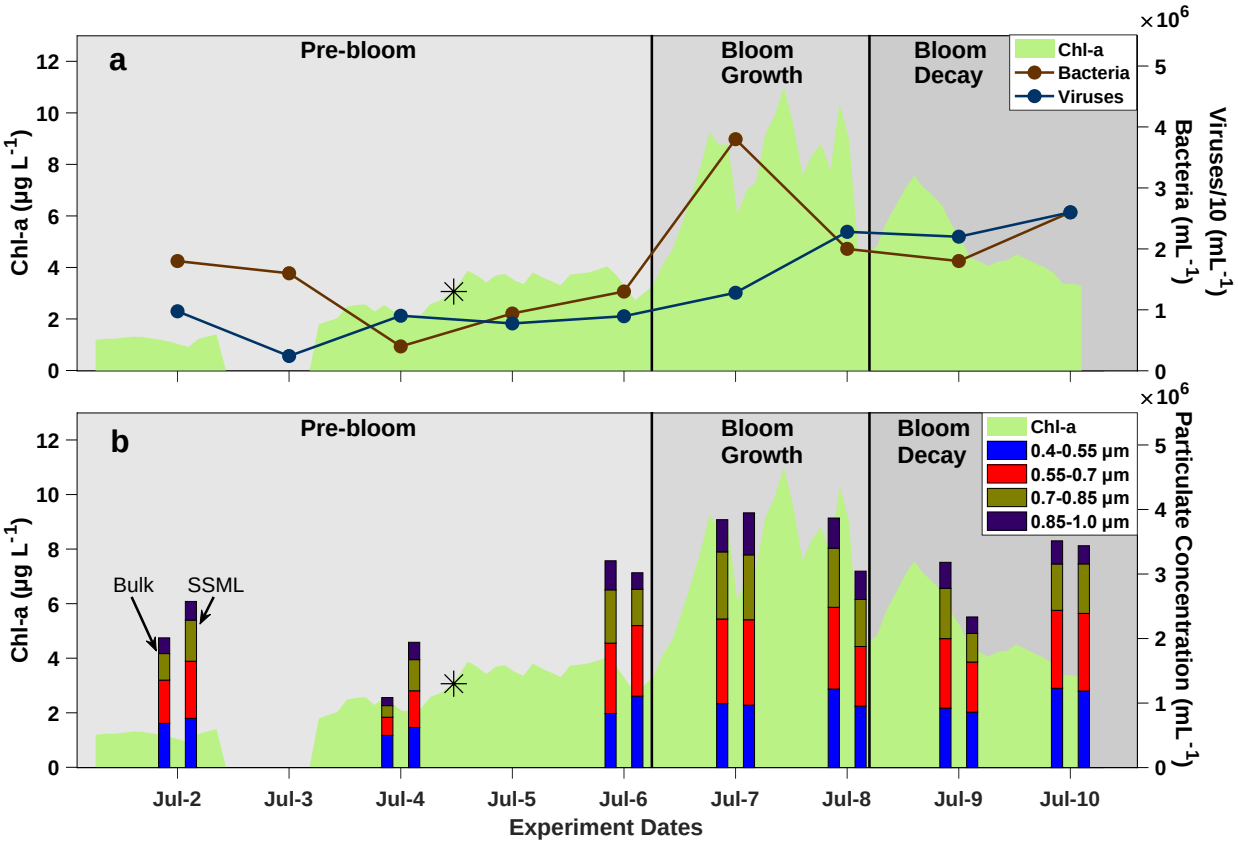


**Figure 2. a)** Development of chl-a, bacteria, and virus concentrations throughout Experiment 1 (asterisk denotes nutrient addition). **b)** SMP concentrations for bulk (left bars) and SSML (right bars) in 0.15 µm size bins (stacked bars) with the full bar height signifying the total SMP concentration. Both plots are divided into pre-bloom, bloom growth, and bloom decay phases (solid lines) based on the beginning of exponential phytoplankton growth (chl-a), and chl-a decaying to half the peak value.

Daily bulk and SSML SMP concentrations are shown as stacked bars in Figure 2b. Both bulk and SSML SMP concentrations were generally higher during the growth and decay phases

compared to the pre-bloom phase. To visualize how different SMP sizes are influenced by the seawater biological activity, the bars in Figure 2b were organized into four size regimes: 0.4-0.55 µm (blue), 0.55-0.7 µm (red), 0.7-0.85 µm (olive), and 0.85-1.0 µm (purple). Daily bulk SMP concentrations for all four size fractions moderately to strongly correlated with daily concentrations of bulk seawater bacteria and chl-a, having Pearson correlation coefficients (r) of 0.64-0.76 and 0.65-0.83, respectively (Table S1). This suggests that bacterial cells contributed to SMPs of all measured sizes, including the microbial mode. Because most phytoplankton are larger than 1 µm, the correlation between SMPs and chl-a is more likely due to direct release of 0.4-1.0 µm algal exudates or aggregation of smaller particulates generated by primary productivity. Also relevant to the microbial mode, virus concentrations showed a strong correlation (r=0.83) with 0.4-0.55 µm particulates (Table S1), suggesting viral lysis of organisms may produce microbial mode SMPs during bloom decay. Overall, the SMP correlations with chl-a, bacteria, and viruses suggest microbial mode formation is controlled by the entire microbial loop with different particulate populations contributing during each bloom phase. To better assess changes in SMP populations throughout the bloom, modal analyses were performed on the pre-bloom, growth, and decay PSDs. Our PSD measurements do not resolve the chemical identity of SMPs, but potential contributors are discussed in the section below.

### 3.3. Potential SMP Populations Contributing to the Microbial Mode

PSD modal analysis reveals the strong resemblance between bulk and SSML PSDs throughout each bloom phase (Figure 3), demonstrating that similar SMP populations are contributing to the microbial mode in the SSML. Specifically, transitioning from the pre-bloom to growth phase, the bulk and SSML PSDs both display large increases in the particulate mode

centered around 0.6-0.7 µm (red). The 0.6-0.7 µm particulate mode has been observed in oceanic measurements of bulk seawater SMPs (Isao et al., 1990; Longhurst et al., 1992; Yamasaki et al., 1998), and is patently visible as the microbial mode labeled in Figure 1.

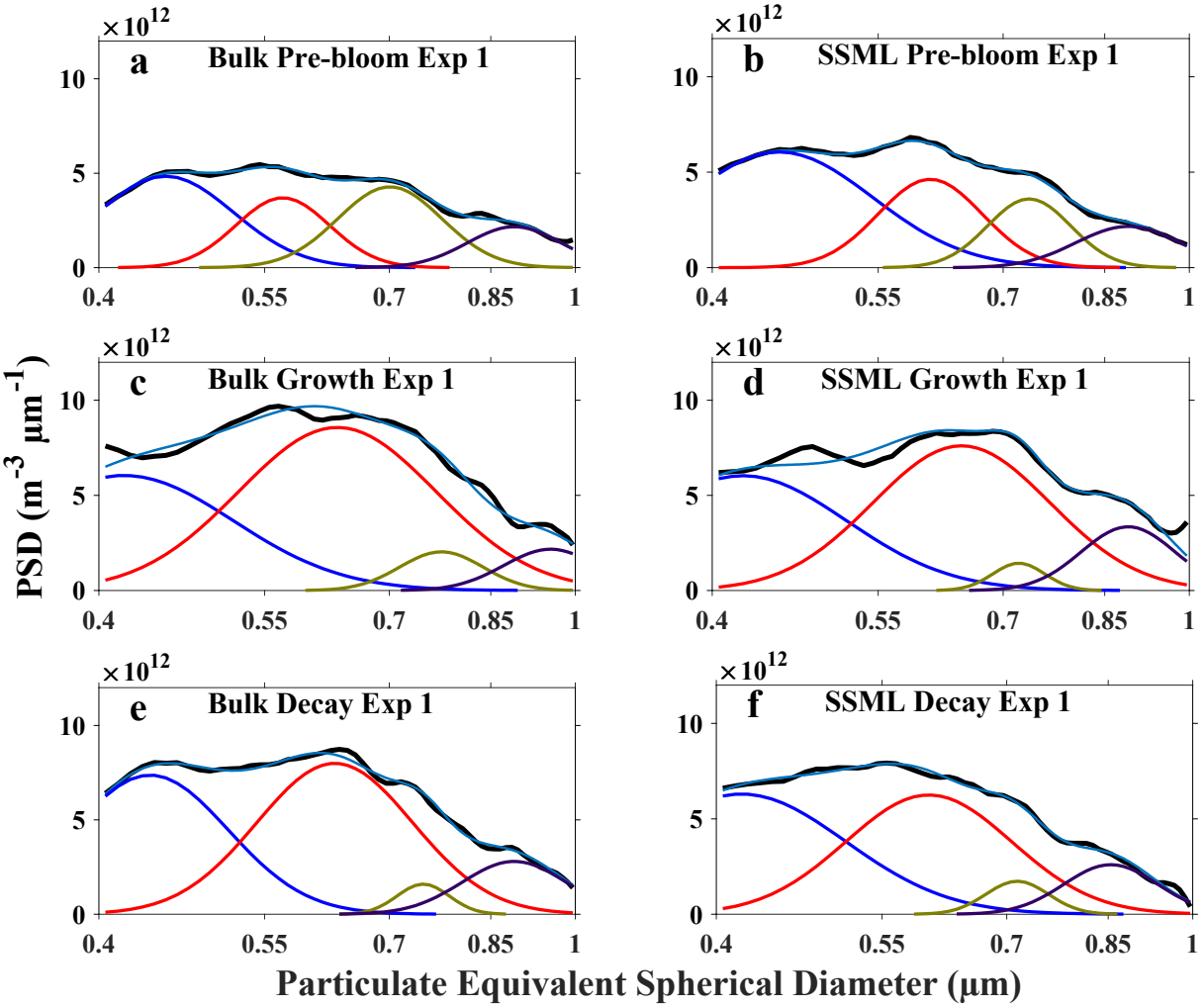


**Figure 3.** A four-component modal analysis of bulk and SSML PSDs for the pre-bloom **(a,b)**, growth **(c,d)**, and decay **(e,f)** phases. The black line is a five-point, centered moving average of the PSDs from each bloom phase. The four modes comprising each PSD are shown in blue, red, olive, and purple with a dark blue line representing the composite of these modes.

As mentioned above, bacteria cells represent one likely contributor to the microbial mode, but sonication experiments have shown that a significant proportion of microbial mode particulates are nonliving organic material (Isao et al., 1990; Yamasaki et al., 1998). Isao et al. (1990) observed that many microbial mode SMPs were hydrated, flexible organic material that aggregated to form larger particulates. Their observations are consistent with submicron-sized nanogels, such as transparent exopolymer particulates (TEP), which are formed through self-assembly and aggregation of dissolved (<0.2 μm) exopolymeric secretions (EPS) from marine phytoplankton and bacteria (Chin et al., 1998; Passow & Alldredge, 1995). This is substantiated by a tentative, but very strong correlation between 0.55-0.7 μm SSML particulates and SSML TEP (>0.4 μm) concentrations in Experiment 1 (Figure S3). Additionally, aggregates of membrane vesicles released by heterotrophic bacteria and cyanobacteria have also been observed in the bulk seawater and SSML (Biller et al., 2014; Patterson et al., 2016). Both of these SMP sources are consistent with the correlation of chl-a and bacteria concentrations to 0.55-0.7 μm bulk SMPs.

The 0.4-0.55 μm SMP concentrations increased during bloom decay and senescence (Figure 3e,f), and closely correlated with elevated virus concentrations. Viral lysis of large marine bacteria can produce smaller particulates with diameters between 0.4-0.7 μm (Shibata et al., 1997), which may represent a source of 0.4-0.55 μm SMPs during bloom decay. Additionally, bacterial egestion by heterotrophic nanoflagellates, which were not measured in this experiment but generally increase following bacteria growth (Nagata & Kirchman, 1992), is known to produce 0.4-0.6 μm picopellets that may contribute to this mode (Nagata, 2000). These observations indicate that further microbial processing of SMPs initially formed by primary production and bacterial growth may alter the identity of particulates comprising the microbial mode.

### 3.4. SMP Partitioning in Seawater and Importance for Ocean-Aerosol Transfer

Stramski et. al (2019) recently reported the first SSML particulate enrichment factors (EFs, Equation 3), calculated from simultaneous, oceanic bulk and SSML PSD measurements on 0.8-50 µm particulates. Their measurements were made in the presence of breaking waves and revealed size-dependent SSML particulate enrichment with larger particulates (>10 µm) having the highest EFs, and enrichment generally decreasing as particulate diameter decreased. For comparison with our SMP measurements, Figure 4 plots a portion of their measured EFs for three separate days in the Santa Barbara Channel (gray lines).

$$\text{Particulate Enrichment Factor (EF)} = \frac{\text{\# of SSML Particulates}}{\text{\# of Bulk Particulates}} \quad (3)$$

Our study extends the measured SMP EF range to 0.4 µm and separates the EFs from both experiments into their biological phases (Figure 4). Both pre-bloom phases displayed only slight SMP enrichment (1.0-1.4), at the low end of 0.8-1.0 µm EF measurements from the Santa Barbara Channel (1.2-2.5, Figure 4). With the exception of one data point, this slight enrichment disappeared during the growth and decay phases, and no SMP enrichment was observed (EF≤1.0). The underlying mechanisms causing lower SMP EFs during the growth and decay phases are uncertain, though one possibility is that the elevated concentrations of biological and organic material in the SSML led to higher particulate aggregation rates (Galgani & Engel, 2016; Verdugo et al., 2004). Faster particulate aggregation could result in a larger proportion of supermicron SSML particulates outside our measurement range.

Overall, the measured EFs (0.7-1.4) show SMP enrichment is slight to nonexistent in this study, consistent with a negligible impact from wave action and bubble formation. Bubble adsorption is a critical process for transporting particulates to the SSML (Crocker et al., 2020; Zhou et al., 1998), and can lead to 5-fold increases in SSML enrichment of biological and organic

particulates (Robinson et al., 2019). Furthermore, Walls & Bird (2017) have found that EF values of yeast cells adsorbed to the bubble film surface increased four-fold, from 5 to 20, as water drained off the film before bursting. Their observations align particulate enrichment with previously observed EFs of 10-22 for bacteria in SSA (Aller et al., 2005; Blanchard & Syzdek, 1982). Thus, the lack of enrichment observed in our study suggests future measurements in wave breaking regimes will be crucial to determine how bubble scavenging and bursting processes impact SMP enrichment in the SSML and transfer into SSA.

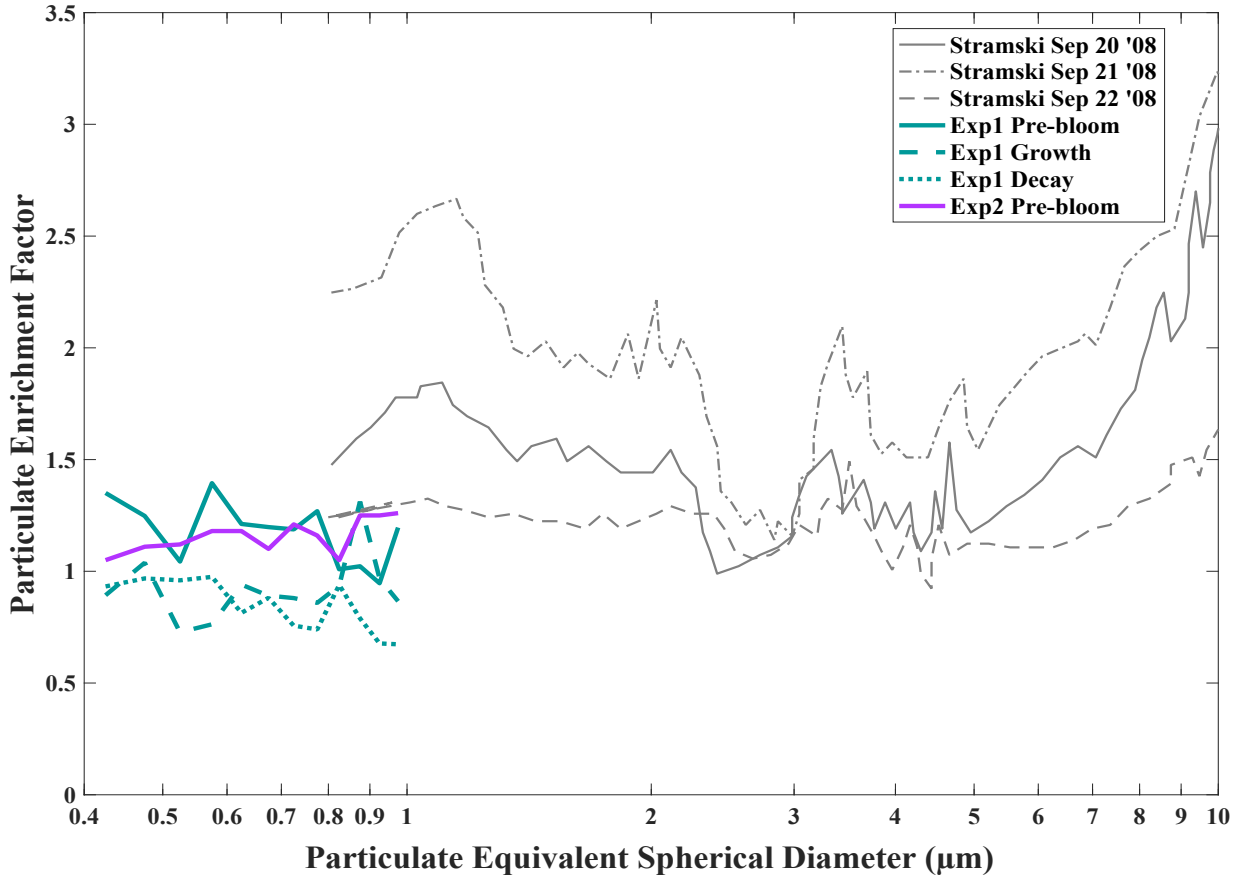


**Figure 4.** SMP enrichment factors from 0.4-1.0 µm in 0.05 µm size bins separated into bloom phases for both experiments. Included for comparison are particulate EFs measured in the Santa Barbara Channel in the presence of breaking waves (gray lines, Stramski et al., 2019).

## 4. Conclusions and Implications for SMP Entrainment in SSA

Herein, we report the first concurrent particulate size distribution measurements of 0.4-1.0 μm SMPs in the bulk seawater and SSML made over the course of two mesocosm experiments. In Experiment 1, which featured a complete phytoplankton bloom cycle, bulk and SSML SMP concentrations were generally higher during the growth and decay phases compared to the pre-bloom phase. This was primarily due to an increase in 0.4-0.7 μm microbial mode SMPs (Figure 2b), with potential biologically-produced particulates in this size range including bacteria cells, algal exudates, nanogels, and vesicle aggregates, among others (Alpert et al., 2011; Patterson et al., 2016). PSD modal analyses further revealed that the particulate populations contributing to the microbial mode depend on the bloom phase (Figure 3). During the growth phase, 0.55-0.7 μm SMPs increased in conjunction with maximum phytoplankton (chl-a) and bacteria abundance. The decay phase was distinguished by increased 0.4-0.55 μm SMPs and virus concentrations, potentially due to cellular debris from viral lysis or grazing of phytoplankton and bacteria during bloom senescence (Azam et al., 1983).

Biologically induced changes in SMP concentrations and distributions may affect particulate entrainment in SSA, which is especially important for SMPs that possess ice nucleating ability. Similar to the SMP concentrations, higher seawater INE concentrations have been reported in biologically-active seawater (Mitts et al., 2021). Moreover, Micro-Raman spectroscopy has demonstrated that biologically-produced SMPs contribute to SSA INPs (McCluskey et al., 2018), and many of the likely microbial mode components have been identified as seawater particulate INEs including heterotrophic bacteria, diatom cell fragments, and potentially nanogels (Alpert et al., 2011; McCluskey et al., 2017; Roy et al., 2021; Wilson et al., 2015). Recent research has shown

that SSA INP concentrations scale with the total aerosol volume (Mitts et al., 2021). Because SSA formed from the bubble's base comprises the majority of SSA volume (Mitts et al., 2021; Prather et al., 2013), the increased bulk SMP concentrations resulting from seawater biological activity may increase the amount of SMP INEs that are transferred into SSA. This may help explain the established connection between elevated seawater biological activity and higher SSA INP concentrations (Creamean et al., 2019; DeMott et al., 2016).

In summary, because seawater particulate concentrations increase with decreasing diameter (Figure 1), submicron INEs may constitute a significant portion of total particulate INEs. Therefore, the increased biological production of SMPs in our experiments, represents one factor that may contribute to higher INE entrainment in SSA during phytoplankton blooms (McCluskey et al., 2018; Mitts et al., 2021). Entrainment of submicron INEs in SSA may be further augmented in wave breaking regimes where bubble scavenging and bursting processes can enhance SMP enrichment in the SSML and transfer into SSA. To assess the contribution of SMPs to SSA INPs, we suggest future experiments on submicron and supermicron SSA INPs that combine size-segregated seawater INE measurements with bulk and SSML PSD measurements. The knowledge gained from this further analysis will help inform climate and weather models working to assess the global radiative balance and precipitation patterns.

## Acknowledgements, Funding Sources, and Data

This work was funded by the National Science Foundation Center for Aerosol Impacts on Chemistry of the Environment (NSF-CAICE), a Center for Chemical Innovation (CHE-1801971). The authors thank the entire SeaSCAPE team, and especially Dr. Kathryn Mayer, Dr. Jon Sauer, Prof. Tim Bertram, and Prof. Chris Cappa for designing and overseeing

the campaign. The authors declare no conflicts of interest or financial conflicts in association with this work. Archiving of the data supporting the conclusions is currently underway and will be publicly available at the time of publication from the UC San Diego Library Digital Collections at: https://doi.org/10.6075/J0SQ90JD.

## References

A. D. McNaught and A. Wilkinson. (2019). *IUPAC. Compendium of Chemical Terminology (the "Gold Book")*. *Blackwell Scientific Publications, Oxford, ISBN 0-9678550-9-8* (2nd ed.). Oxford.

Aller, J. Y., Kuznetsova, M. R., Jahns, C. J., & Kemp, P. F. (2005). The sea surface microlayer as a source of viral and bacterial enrichment in marine aerosols. *Journal of Aerosol Science*, *36*(5–6), 801–812. https://doi.org/10.1016/j.jaerosci.2004.10.012

Alpert, P. A., Aller, J. Y., & Knopf, D. A. (2011). Ice nucleation from aqueous NaCl droplets with and without marine diatoms. *Atmospheric Chemistry and Physics*, *11*(12), 5539–5555. https://doi.org/10.5194/acp-11-5539-2011

Azam, F., Fenchel, T., Field, J., Gray, J., Meyer-Reil, L., & Thingstad, F. (1983). The Ecological Role of Water-Column Microbes in the Sea. *Marine Ecology Progress Series*, *10*, 257–263. https://doi.org/10.3354/meps010257

Babin, M., Stramski, D., Reynolds, R. A., Wright, V. M., & Leymarie, E. (2012). Determination of the volume scattering function of aqueous particle suspensions with a laboratory multi-

angle light scattering instrument. *Applied Optics*, *51*(17), 3853–3873. https://doi.org/10.1364/AO.51.003853

Bigg, E. K., & Leck, C. (2001). Cloud-active particles over the central Arctic Ocean. *Journal of Geophysical Research*, *106*(D23), 32,155-32,166.

Bigg, E. K., & Leck, C. (2008). The composition of fragments of bubbles bursting at the ocean surface. *Journal of Geophysical Research Atmospheres*, *113*(11), 1–7. https://doi.org/10.1029/2007JD009078

Bigg, E. K., Leck, C., & Tranvik, L. (2004). Particulates of the surface microlayer of open water in the central Arctic Ocean in summer. *Marine Chemistry*, *91*(1–4), 131–141. https://doi.org/10.1016/j.marchem.2004.06.005

Biller, S. J., Schubotz, F., Roggensack, S. E., Thompson, A. W., Summons, R. E., & Chisholm, S. W. (2014). Bacterial vesicles in marine ecosystems. *Science*, *343*(6167), 183–186. https://doi.org/10.1126/science.1243457

Blanchard, D. C., & Syzdek, L. D. (1982). Water-to-air transfer and enrichment of bacteria in drops from bursting bubbles. *Applied and Environmental Microbiology*, *43*(5), 1001–1005. https://doi.org/10.1128/aem.43.5.1001-1005.1982

Brussaard, C. P. D. (2004). Optimization of Procedures for Counting Viruses by Flow Cytometry. *Applied and Environmental Microbiology*, *70*(3), 1506–1513. https://doi.org/10.1128/AEM.70.3.1506-1513.2004

Carlson, D. J. (1982). Surface microlayer phenolic enrichments indicate sea surface slicks. *Nature*, *296*(5856), 426–429. https://doi.org/10.1038/296426a0

Chin, W. C., Orellana, M. V., & Verdugo, P. (1998). Spontaneous assembly of marine dissolved organic matter into polymer gels. *Nature*, *391*(6667), 568–572. https://doi.org/10.1038/35345

Creamean, J. M., Cross, J. N., Pickart, R., McRaven, L., Lin, P., Pacini, A., et al. (2019). Ice Nucleating Particles Carried From Below a Phytoplankton Bloom to the Arctic Atmosphere. *Geophysical Research Letters*, *46*(14), 8572–8581. https://doi.org/10.1029/2019GL083039

Crocker, Daniel R.; Deane, Grant B.; Cao, Ruochen; Santander, Mitchell V.; Morris, Clare K.; Mitts, Brock A.; Dinasquet, Julie; Amiri, Sarah; Malfatti, Francesca; Prather, Kimberly A.; Thiemens, Mark H. (2021). Data from: Biologically Induced Changes in the Partitioning of Submicron Particulates Between Bulk Seawater and the Sea Surface Microlayer. In Center for Aerosol Impacts on Chemistry of the Environment (CAICE). UC San Diego Library Digital Collections. https://doi.org/10.6075/J0SQ90JD

Crocker, D. R., Hernandez, R. E., Huang, H. D., Pendergraft, M. A., Cao, R., Dai, J., et al. (2020). Biological Influence on d13C and Organic Composition of Nascent Sea Spray Aerosol. *ACS Earth and Space Chemistry*, *4*(9), 1686–1699. https://doi.org/10.1021/acsearthspacechem.0c00072

Cunliffe, M., & Wurl, O. (2015). Sampling the Sea Surface Microlayer (pp. 255–261). https://doi.org/10.1007/8623_2015_83

DeMott, P. J., Hill, T. C. J., McCluskey, C. S., Prather, K. A., Collins, D. B., Sullivan, R. C., et al. (2016). Sea spray aerosol as a unique source of ice nucleating particles. *Proceedings of the National Academy of Sciences of the United States of America*, *113*(21), 5797–5803. https://doi.org/10.1073/pnas.1514034112

Després, V. R., Alex Huffman, J., Burrows, S. M., Hoose, C., Safatov, A. S., Buryak, G., et al. (2012). Primary biological aerosol particles in the atmosphere: A review. *Tellus, Series B: Chemical and Physical Meteorology*, *64*(1). https://doi.org/10.3402/tellusb.v64i0.15598

Einstein, A. (1905). Über die von der molekularkinetischen Theorie der Wärme geforderte Bewegung von in ruhenden Flüssigkeiten suspendierten Teilchen. *Annalen Der Physik*, *322*(8), 549–560. https://doi.org/10.1002/andp.19053220806

Engel, A. (2009). Determination of Marine Gel Particles. In *Practical Guidelines for the Analysis of Seawater*. https://doi.org/10.1201/9781420073072.ch7

Facchini, M. C., Rinaldi, M., Decesari, S., Carbone, C., Finessi, E., Mircea, M., et al. (2008). Primary submicron marine aerosol dominated by insoluble organic colloids and aggregates. *Geophysical Research Letters*, *35*(17). https://doi.org/10.1029/2008GL034210

Galgani, L., & Engel, A. (2016). Changes in optical characteristics of surface microlayers hint to photochemically and microbially mediated DOM turnover in the upwelling region off the coast of Peru. *Biogeosciences*, *13*(8), 2453–2473. https://doi.org/10.5194/bg-13-2453-2016

Gallego-Urrea, J. A., Tuoriniemi, J., Pallander, T., & Hassellöv, M. (2010). Measurements of nanoparticle number concentrations and size distributions in contrasting aquatic environments using nanoparticle tracking analysis. *Environmental Chemistry*, *7*(1), 67–81. https://doi.org/10.1071/EN09114

Gasol, J. M., & Del Giorgio, P. A. (2000). Using flow cytometry for counting natural planktonic bacteria and understanding the structure of planktonic bacterial communities. *Scientia Marina*, *64*(2), 197–224. https://doi.org/10.3989/scimar.2000.64n2197

Groundwater, H., Twardowski, M. S., Dierssen, H. M., Sciandra, A., & Freeman, S. A. (2012). Determining size distributions and composition of particles suspended in water: A new SEM-EDS protocol with validation and comparison to other methods. *Journal of Atmospheric and Oceanic Technology*, *29*(3), 433–449. https://doi.org/10.1175/JTECH-D-11-00026.1

Guillard, R. R. L., & Ryther, J. H. (1962). Studies of marine planktonic diatoms. I. Cyclotella nana. *Canadian Journal of Microbiology*, *8*, 229–239.

Holm-Hansen, O., Lorenzen, C. J., Holmes, R. W., & Strickland, J. D. H. (1965). Fluorometric determination of chlorophyll. *ICES Journal of Marine Science*, *30*(1), 3–15. https://doi.org/10.1093/icesjms/30.1.3

Isao, K., Hara, S., Terauchi, K., & Kogure, K. (1990). Role of sub-micrometre particles in the ocean. *Nature*, *345*(6272), 242–244. https://doi.org/10.1038/345242a0

Jonasz, M., & Fournier, G. (1996). Approximation of the size distribution of marine particles by a sum of log-normal functions. *Limnology and Oceanography*, *41*(4), 744–754. https://doi.org/10.4319/lo.1996.41.4.0744

Jonasz, M., & Fournier, G. R. (2007). *Light Scattering by Particles in Water: Theoretical and Experimental Foundations*. *Light Scattering by Particles in Water: Theoretical and Experimental Foundations* (1st ed.). Academic Press. https://doi.org/10.1016/B978-0-12-388751-1.X5000-5

Knopf, D. A., Alpert, P. A., Wang, B., & Aller, J. Y. (2011). Stimulation of ice nucleation by marine diatoms. *Nature Geoscience*, *4*(2), 88–90. https://doi.org/10.1038/ngeo1037

Leck, C., & Bigg, E. K. (2005). Biogenic particles in the surface microlayer and overlaying atmosphere in the central Arctic Ocean during summer. *Tellus, Series B: Chemical and Physical Meteorology*, *57*(4), 305–316. https://doi.org/10.1111/j.1600-0889.2005.00148.x

Lee, C., Sultana, C. M., Collins, D. B., Santander, M. V., Axson, J. L., Malfatti, F., et al. (2015). Advancing Model Systems for Fundamental Laboratory Studies of Sea Spray Aerosol Using the Microbial Loop. *Journal of Physical Chemistry A*, *119*(33), 8860–8870. https://doi.org/10.1021/acs.jpca.5b03488

Longhurst, A. R., Koike, I., Li, W. K. W., Rodriguez, J., Dickie, P., Kepay, P., et al. (1992). Sub-micron particles in northwest Atlantic shelf water. *Deep Sea Research Part A, Oceanographic Research Papers*, *39*(1), 1–7. https://doi.org/10.1016/0198-0149(92)90016-M

Marie, D., Partensky, F., Jacquet, S., & Vaulot, D. (1997). Enumeration and cell cycle analysis of natural populations of marine picoplankton by flow cytometry using the nucleic acid stain SYBR Green I. *Applied and Environmental Microbiology*, *63*(1), 186–193. https://doi.org/10.1128/aem.63.1.186-193.1997

McCluskey, C. S., Hill, T. C. J., Malfatti, F., Sultana, C. M., Lee, C., Santander, M. V., et al. (2017). A dynamic link between ice nucleating particles released in nascent sea spray aerosol and oceanic biological activity during two mesocosm experiments. *Journal of the Atmospheric Sciences*, *74*(1), 151–166. https://doi.org/10.1175/JAS-D-16-0087.1

McCluskey, C. S., Hill, E. T. C. J., Sultana, C. M., Laskina, O., Trueblood, J., Santander, M. V., et al. (2018). A mesocosm double feature: Insights into the chemical makeup of marine ice nucleating particles. *Journal of the Atmospheric Sciences*, *75*(7), 2405–2423.

https://doi.org/10.1175/JAS-D-17-0155.1

Mitts, B. A., Wang, X., Lucero, D. D., Beall, C. M., Deane, G. B., DeMott, P. J., & Prather, K. A. (2021). Importance of Supermicron Ice Nucleating Particles in Nascent Sea Spray. *Geophysical Research Letters*, *48*(3). https://doi.org/10.1029/2020GL089633

Moore, D. S., Notz, W. I., & Flinger, M. A. (2013). *The Basic Practice of Statistics (6th ed.) and Correlation*. *Freeman and Company*.

Nagata, T., & Kirchman, D. L. (1992). Release of macromolecular organic complexes by heterotrophic marine flagellates. *Marine Ecology Progress Series*, *83*(2–3), 233–240. https://doi.org/10.3354/meps083233

Nagata, Toshi. (2000). "Picopellets" Produced by Phagotrophic Nanoflagellates: Role in the Material Cycling within Marine Environments (pp. 241–256). https://doi.org/10.1007/978-94-017-1319-1_12

Noble, R. T., & Fuhrman, J. A. (1998). Use of SYBR Green I for rapid epifluorescence counts of marine viruses and bacteria. *Aquatic Microbial Ecology*, *14*(2), 113–118. https://doi.org/10.3354/ame014113

Orellana, M. V., Matrai, P. A., Leck, C., Rauschenberg, C. D., Lee, A. M., & Coz, E. (2011). Marine microgels as a source of cloud condensation nuclei in the high arctic. *Proceedings of the National Academy of Sciences of the United States of America*, *108*(33), 13612–13617. https://doi.org/10.1073/pnas.1102457108

Palumbo, A. V., Ferguson, R. L., & Rublee, P. A. (1984). Size of suspended bacterial cells and association of heterotrophic activity with size fractions of particles in estuarine and coastal

waters. *Applied and Environmental Microbiology*, *48*(1), 157–164. https://doi.org/10.1128/aem.48.1.157-164.1984

Passow, U. (2002). Transparent exopolymer particles (TEP) in aquatic environments. *Progress in Oceanography*. https://doi.org/10.1016/S0079-6611(02)00138-6

Passow, U., & Alldredge, A. L. (1995). A dye-binding assay for the spectrophotometric measurement of transparent exopolymer particles (TEP). *Limnology and Oceanography*. https://doi.org/10.4319/lo.1995.40.7.1326

Patterson, J. P., Collins, D. B., Michaud, J. M., Axson, J. L., Sultana, C. M., Moser, T., et al. (2016). Sea spray aerosol structure and composition using cryogenic transmission electron microscopy. *ACS Central Science*, *2*(1), 40–47. https://doi.org/10.1021/acscentsci.5b00344

Prather, K. A., Bertram, T. H., Grassian, V. H., Deane, G. B., Stokes, M. D., DeMott, P. J., et al. (2013). Bringing the ocean into the laboratory to probe the chemical complexity of sea spray aerosol. *Proceedings of the National Academy of Sciences of the United States of America*, *110*(19), 7550–7555. https://doi.org/10.1073/pnas.1300262110

Reynolds, R. A., Stramski, D., Wright, V. M., & Woźniak, S. B. (2010). Measurements and characterization of particle size distributions in coastal waters. *Journal of Geophysical Research: Oceans*, *115*(8). https://doi.org/10.1029/2009JC005930

Robinson, T. B., Giebel, H. A., & Wurl, O. (2019). Riding the plumes: Characterizing bubble scavenging conditions for the enrichment of the sea-surface microlayer by transparent exopolymer particles. *Atmosphere*, *10*(8). https://doi.org/10.3390/atmos10080454

Roy, P., Mael, L. E., Hill, T. C. J., Mehndiratta, L., Peiker, G., House, M. L., et al. (2021). Ice Nucleating Activity and Residual Particle Morphology of Bulk Seawater and Sea Surface Microlayer. *ACS Earth and Space Chemistry*. https://doi.org/10.1021/acsearthspacechem.1c00175

Runyan, H., Reynolds, R. A., & Stramski, D. (2020). Evaluation of Particle Size Distribution Metrics to Estimate the Relative Contributions of Different Size Fractions Based on Measurements in Arctic Waters. *Journal of Geophysical Research: Oceans*, *125*(6). https://doi.org/10.1029/2020JC016218

Shibata, A., Kogure, K., Koike, I., & Ohwada, K. (1997). Formation of submicron colloidal particles from marine bacteria by viral infection. *Marine Ecology Progress Series*, *155*, 303–307. https://doi.org/10.3354/meps155303

Singh, P., Bodycomb, J., Travers, B., Tatarkiewicz, K., Travers, S., Matyas, G. R., & Beck, Z. (2019). Particle size analyses of polydisperse liposome formulations with a novel multispectral advanced nanoparticle tracking technology. *International Journal of Pharmaceutics*, *566*, 680–686. https://doi.org/10.1016/j.ijpharm.2019.06.013

Stramski, D., Reynolds, R. A., Gernez, P., Röttgers, R., & Wurl, O. (2019). Inherent optical properties and particle characteristics of the sea-surface microlayer. *Progress in Oceanography*, *176*. https://doi.org/10.1016/j.pocean.2019.05.009

Tesson, S. V. M., & Šantl-Temkiv, T. (2018). Ice nucleation activity and aeolian dispersal success in airborne and aquatic microalgae. *Frontiers in Microbiology*, *9*(NOV), 1–14. https://doi.org/10.3389/fmicb.2018.02681

Utermöhl, H. (1958). Zur Vervollkommnung der quantitativen Phytoplankton-Methodik. *SIL Communications, 1953-1996*, *9*(1), 1–38. https://doi.org/10.1080/05384680.1958.11904091

Verdugo, P. (2012). Marine microgels. *Annual Review of Marine Science*, *4*, 375–400. https://doi.org/10.1146/annurev-marine-120709-142759

Verdugo, P., Alldredge, A. L., Azam, F., Kirchman, D. L., Passow, U., & Santschi, P. H. (2004). The oceanic gel phase: A bridge in the DOM-POM continuum. In *Marine Chemistry* (Vol. 92, pp. 67–85). https://doi.org/10.1016/j.marchem.2004.06.017

Walls, P. L. L., & Bird, J. C. (2017). Enriching particles on a bubble through drainage: Measuring and modeling the concentration of microbial particles in a bubble film at rupture. *Elementa*, *5*. https://doi.org/10.1525/elementa.230

Wang, X., Deane, G. B., Moore, K. A., Ryder, O. S., Stokes, M. D., Beall, C. M., et al. (2017). The role of jet and film drops in controlling the mixing state of submicron sea spray aerosol particles. *Proceedings of the National Academy of Sciences of the United States of America*, *114*(27), 6978–6983. https://doi.org/10.1073/pnas.1702420114

Wells, M. L., & Goldberg, E. D. (1992). Marine submicron particles. *Marine Chemistry*, *40*(1–2), 5–18. https://doi.org/10.1016/0304-4203(92)90045-C

Wells, M. L., & Goldberg, E. D. (1994). The distribution of colloids in the North Atlantic and Southern Oceans. *Limnology and Oceanography*, *39*(2), 286–302. https://doi.org/10.4319/lo.1994.39.2.0286

Wilson, T. W., Ladino, L. A., Alpert, P. A., Breckels, M. N., Brooks, I. M., Browse, J., et al.

(2015). A marine biogenic source of atmospheric ice-nucleating particles. *Nature*, *525*(7568), 234–238. https://doi.org/10.1038/nature14986

Wolf, M. J., Goodell, M., Dong, E., Dove, L. A., Zhang, C., Franco, L. J., et al. (2020). A link between the ice nucleation activity and the biogeochemistry of seawater. *Atmospheric Chemistry and Physics*, *20*(23), 15341–15356. https://doi.org/10.5194/acp-20-15341-2020

Wurl, O., Wurl, E., Miller, L., Johnson, K., & Vagle, S. (2011). Formation and global distribution of sea-surface microlayers. *Biogeosciences*, *8*(1), 121–135. https://doi.org/10.5194/bg-8-121-2011

Yamasaki, A., Fukuda, H., Fukuda, R., Miyajima, T., Nagata, T., Ogawa, H., & Koike, I. (1998). Submicrometer particles in northwest Pacific coastal environments: Abundance, size distribution, and biological origins. *Limnology and Oceanography*, *43*(3), 536–542. https://doi.org/10.4319/lo.1998.43.3.0536

Zhang, X., Twardowski, M., & Lewis, M. (2011). Retrieving composition and sizes of oceanic particle subpopulations from the volume scattering function. *Applied Optics*, *50*(9), 1240–1259. https://doi.org/10.1364/AO.50.001240

Zhang, X., Gray, D. J., Huot, Y., You, Y., & Bi, L. (2012). Comparison of optically derived particle size distributions: Scattering over the full angular range versus diffraction at near forward angles. *Applied Optics*, *51*(21), 5085–5099. https://doi.org/10.1364/AO.51.005085

Zhou, J., Mopper, K., & Passow, U. (1998). The role of surface-active carbohydrates in the formation of transparent exopolymer particles by bubble adsorption of seawater. *Limnology and Oceanography*, *43*(8), 1860–1871. https://doi.org/10.4319/lo.1998.43.8.1860